Calculations in the $50 < N$, $Z < 82$ region with an interaction derived from the Tabakin potential

N. de Takacsy and S. Das Gupta

Physics Department, McGill University, P. O. Box 6070, Station "A", Montreal, Quebec, Canada H3C 3G1
(Received 23 June 1975; revised manuscript received 8 September 1975)

The region of the Periodic Table with $50 \leq Z$, $N \leq 82$ is studied using fixed single particle energies and a semirealistic effective interaction derived from the Tabakin potential. All the free parameters are determined by fitting the data on the odd-mass Sn isotopes and $N = 82$ isotones. A conventional quasiparticle formalism is then used to study the structure of a range of spherical nuclei near the $N = 82$ and the $Z = 50$ magic numbers. A deformed Hartree-Fock plus BCS method is used to obtain the structure and electromagnetic properties of deformed nuclei, particularly the neutron-deficient even Ba isotopes. Prolate deformation is found to be favored. In the Ba isotopes, although neutrons have BCS correlation, the protons develop an energy gap between occupied and unoccupied orbitals due to the Hartree-Fock field itself. The proton orbitals are then tested through spectroscopic calculations in La isotopes. Both for spherical and deformed nuclei, agreement between theory and experiment is very satisfactory.

> NUCLEAR STRUCTURE Mass region $100 < A < 150$; calculated levels, J, π, and other properties. Semirealistic forces; combination of deformed Hartree-Fock and BCS methods.

I. INTRODUCTION

In recent years, a great deal of experimental information has become available on nuclei in the $50 \leq Z$, $N \leq 82$ region of the Periodic Table. Of particular interest are the results of the Berkeley group and their collaborators,[1,2] which show that the neutron deficient La and Ba isotopes have prolate rather than oblate deformation. The older calculations[3,4] for this region had generally tended to favor oblate shapes, but the newer calculations[5-8] indicate that these nuclei are generally γ-soft, so that examples of oblate, prolate, or triaxial slopes all occur.

This deformed region is framed by the spherical nuclei near the $Z = 50$ and the $N = 82$ magic numbers. The Sn isotopes and their immediate neighbors have been extensively studied and the results are reviewed by Baranger[9]; more recent calculations have also been reported.[10] A number of calculations on the $N = 82$ isotones have also been reported.[11,12]

The various calculations mentioned above are based on quite different theoretical approaches. The calculations for the Sn region[9,10] use a quasiparticle formalism with realistic interactions and a 12-orbital space. Those for the $N = 82$ isotopes are done in a five-orbital space with empirical residual interactions and either a quasiparticle[11] or a shell model[12] formalism. The calculations for the deformed region also use a variety of formalisms; a typical example is that of Ragnarsson *et al.*,[5] who use a deformed oscillator potential and a pairing force to calculate the shell corrections to the liquid drop energy using the Strutinsky prescription.

The present work is intended to show that it is possible to study the structure and properties of both the spherical and deformed nuclei in this region using a five-orbital space with fixed single particle energies and matrix elements derived from the Tabakin potential.[13] The spherical nuclei are treated using a conventional quasiparticle formalism, and the deformed nuclei with a combination of deformed Hartree-Fock and BCS methods. All the free parameters are determined, once and for all, by fitting the one-quasiparticle states in the odd-mass Sn isotopes and $N = 82$ isotones. The rest of the calculations are then absolute in the sense that no parameters remain.

II. VALENCE SPACE AND THE EFFECTIVE INTERACTION

Since we are interested in a large number of nuclei, it is necessary to limit the valence space as much as possible. Both protons and neutrons are therefore restricted to the five orbitals between the magic numbers 50 and 82: these are the $1d_{5/2}$, $0g_{7/2}$, $2s_{1/2}$, $1d_{3/2}$, and $0h_{11/2}$ orbitals. Then the shell model Hamiltonian is

$$H = \sum_{\alpha} \epsilon_\alpha a_\alpha^\dagger a_\alpha + \tfrac{1}{4} \sum_{\alpha\beta\gamma\delta} v_{\alpha\beta\gamma\delta} a_\alpha^\dagger a_\beta^\dagger a_\delta a_\gamma, \qquad (1)$$

where the single particle energies ϵ_α include the kinetic energy and the one-body potential due to

the ^{100}Sn core, and the residual interaction be-
tween valence particles determines the matrix
elements $v_{\alpha\beta\gamma\delta}$. The neutron single particle en-
ergies are obtained by fitting the one-quasiparticle
states in the odd-mass Sn isotopes and, similarly,
the proton single particle energies are determined
by the spectra of the odd-mass $N = 82$ isotones.
The details are discussed in subsequent sections,
and the results are shown in Table I.

The residual interaction is constructed starting
from the Tabakin potential.[13] The bare potential
is first renormalized by including the second
order ladder graph. This is done in the relative
coordinate system, using an oscillator averaged
approximation to the Pauli operator.[14] Then this
partially renormalized interaction is used to cal-
culate core-polarization corrections to the matrix
elements.[15] Only the "0 $\hbar\omega$" particle-hole excita-
tions were included, assuming a ^{100}Sn core: i.e.,
the hole was restricted to the $g_{9/2}$ orbital and the
particle to any of the five valence orbitals. The
energy denominator for all the core-polarization
graphs was taken to be a constant 8.1 MeV. All
the radial integrals are calculated with an oscil-
lator constant $\hbar\omega = 8.1$ MeV. Obviously, this
renormalization scheme (illustrated in Fig. 1) is
reasonable but not completely adequate; for ex-
ample, the "1$\hbar\omega$" and "2$\hbar\omega$" core-polarization
contributions are not included, even though they
are known to be important in other regions of the
Periodic Table.[14-18] We therefore feel free to
modify selected matrix elements in order to im-
prove the agreement with data. The needed mod-
ifications turn out to be rather minor, and are
listed below together with the corresponding
physical motivation; the resulting improvements
in the calculated nuclear properties are shown in
later sections.

Inspection of the $J = 0$, $T = 1$ matrix elements
shows that the pairing in the $(h_{11/2})^2$ configuration
is considerably weaker than what a pure pairing
force would predict, while the pairing in the
$(s_{1/2})^2$ configuration is much stronger. Since
pairing forces have been used with some success
in this region, we arbitrarily multiply all the
diagonal $(h_{11/2})^2$ $T = 1$ matrix elements by 1.3 and
the diagonal $(s_{1/2})^2$ $T = 1$ matrix element by 0.8.
These changes result in slightly improved spectra
for the Sn isotopes. Again, in a pairing plus
quadrupole model, the proton pairing force is
usually taken to be somewhat stronger than the
neutron pairing force; presumably this comes
about because there are more neutrons than pro-
tons in the nuclei being studied, so that the core-
polarization contribution (which has a very strong
effect on the $J = 0$ matrix elements) is bigger for
protons than for neutrons. Since we calculate

TABLE I. The single particle energies in MeV.

	$1d_{5/2}$	$0g_{7/2}$	$2s_{1/2}$	$1d_{3/2}$	$0h_{11/2}$
Protons	0.35	0	2.00	2.30	3.00
Neutrons	0	0.10	1.70	2.35	2.90

core polarization using a ^{100}Sn core, this effect
is not included in our matrix elements. We there-
fore add to the effective proton-proton interaction
an extra pairing contribution, the strength of
which is $G_p = 0.03$ MeV fm^{-3}, as deduced from the
differences between the proton and neutron pairing
forces used in Ref. 4. This results in a modest
increase in the proton pairing matrix elements
and produces better agreement with the experi-
mental odd-even mass differences.

In addition to the nuclear effective interaction,
constructed as above, the two-body Coulomb po-
tential was explicitly included. This does not
significantly alter any of the physically interesting
properties; however, Coulomb effects must be
included, one way or another, when calculating
the odd-even mass differences along an isotone
chain.

The matrix elements and single particle ener-
gies, once determined, are held constant for the
entire region of interest, i.e., typically from
^{110}Sn to ^{146}Gd, both for spherical and for deformed
nuclei. This has one disadvantage which arises
from the poor saturation characteristics of the
Tabakin potential[14]: although the predicted binding
energy at the experimental density agrees well
with experiment, saturation occurs at roughly
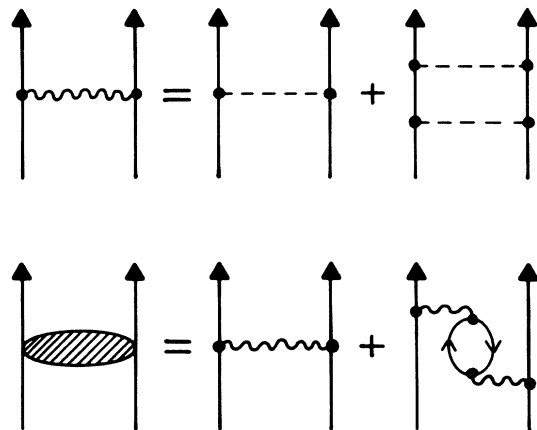twice nuclear density and at much too large a

FIG. 1. The effective interaction is obtained from
the bare potential by including the second order ladder
graphs and the "0$\hbar\omega$" core-polarization corrections.

TABLE II. The G and F matrix elements of the full effective interaction. The definition is $G(\alpha, \beta, J = 0)$ $= G(\alpha, \beta, J = 0)_{\text{Baranger}}/[(j_\alpha + \frac{1}{2})(j_\beta + \frac{1}{2})]^{1/2}$, and similarly for $F(\alpha, \beta, J = 0)$.

	$d_{5/2}$	$g_{7/2}$	$s_{1/2}$	$d_{3/2}$	$h_{11/2}$
$G(p\text{-}p)$	0.156	0.219	0.204	0.393	0.141
	0.219	0.109	0.170	0.179	0.344
	0.204	0.170	0.387	0.224	0.141
	0.393	0.179	0.224	0.039	0.200
	0.141	0.344	0.141	0.200	0.136
$G(n\text{-}n)$	0.226	0.193	0.192	0.376	0.119
	0.193	0.158	0.145	0.159	0.319
	0.192	0.145	0.637	0.211	0.115
	0.376	0.159	0.211	0.152	0.174
	0.119	0.319	0.115	0.174	0.157
$F(p\text{-}p)$	−0.025	−0.109	−0.012	0.038	−0.112
	−0.109	−0.167	−0.154	−0.197	0.075
	−0.012	−0.154	0.193	−0.071	−0.102
	0.038	−0.197	−0.071	−0.091	−0.054
	−0.112	0.075	−0.102	−0.054	−0.078
$F(p\text{-}n)$	0.567	0.333	0.554	0.659	0.345
	0.333	0.425	0.284	0.319	0.590
	0.554	0.284	1.188	0.463	0.312
	0.659	0.319	0.463	0.448	0.373
	0.345	0.590	0.312	0.373	0.445
$F(n\text{-}n)$	0.180	0.139	0.241	0.293	0.122
	0.139	0.044	0.093	0.048	0.316
	0.241	0.093	0.318	0.182	0.132
	0.293	0.048	0.182	0.090	0.181
	0.122	0.316	0.132	0.181	0.128

binding energy. Since the $(sdg + h_{11/2})$ shell is filled without decreasing $\hbar\omega$, the density increases with increasing A, and therefore the predicted binding energy increases with A much faster than the experimental binding energy. As it turns out, this does not affect any physical properties except the curve of separation energy vs particle number, and therefore these poor saturation characteristics are not a serious problem.

III. SPHERICAL NUCLEI AND DETERMINATION OF THE PARAMETERS

The neutron single particle energies are determined by fitting the spectra of the odd-mass Sn isotopes using a BCS method, including blocking. Initially we tried this with the renormalized matrix element obtained from the Tabakin potential without arbitrary modifications. Although the results were generally reasonable, it was found difficult to keep the $2s_{1/2}$ quasiparticle state as the ground state for ^{117}Sn and ^{119}Sn, presumably because the pairing in the $2s_{1/2}$ orbital was too strong compared to the pairing in the $0h_{11/2}$ orbi-

tal. We therefore modified the effective force by multiplying the diagonal, $T = 1$, $h_{11/2}{}^2$ matrix elements by 1.3 and the diagonal, $T = 1$, $s_{1/2}{}^2$ matrix element by 0.8. The actual values 1.3 and 0.8 are to some extent arbitrary since we did not really investigate other possibilities. With this modification we obtain the single neutron energies given in Table I. The resulting one-quasiparticle spectra are compared to experiment[9,18] in Fig. 2. Generally, the fit is comparable to that obtained by other similar calculations,[9, 10, 19] typically done using a larger space. The odd-even mass differences are obtained from the ground state energies of the odd-mass nuclei and the ground state energies of the even nuclei (obtained by a normal BCS calculation). The results are compared to experiment[20] in Fig. 3. The agreement is good on the average but we (like others before us) fail to reproduce the interesting dip at $A = 115$. It is worth pointing out that three-quasiparticle states, presumably related to the first 2^+ state of the adjacent even-even nuclei, appear at excitation $\gtrsim 1$ MeV.

The proton single particle energies are determined in the same way, using the $N = 82$ isotones. The final modification of the effective interaction was made at this stage to improve the theoretical odd-even mass differences which otherwise would have been too small by ~100 keV: we add an extra proton pairing force with a strength $G_p = 0.03$ MeV. This corresponds roughly to the difference in the proton and neutron pairing forces used by
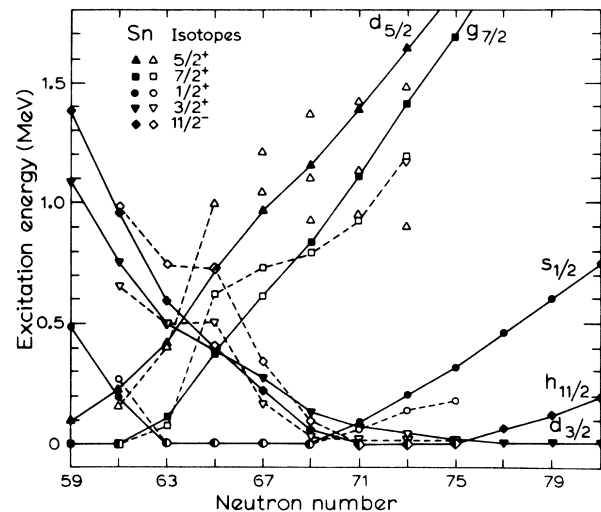

FIG. 2. The one neutron quasiparticle states in the Sn isotopes. The open symbols and the dashed lines refer to experiment, while the solid symbols joined by solid lines are the results of the BCS calculation with blocking.
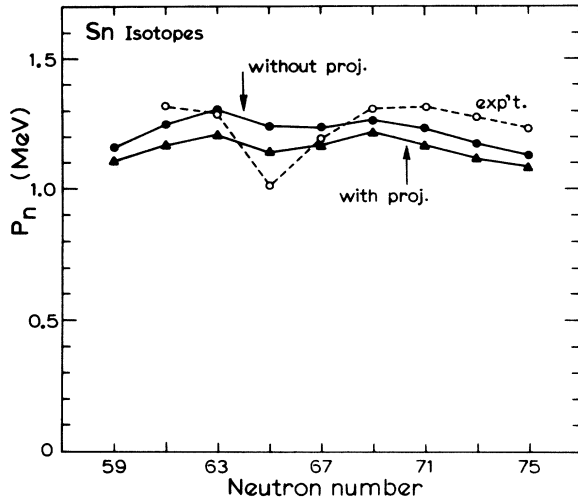
FIG. 3. The odd-even mass differences for the Sn isotopes. The open circles joined by a dashed line are the experimental results. The solid circles represent the results of the BCS calculation including blocking for the odd-mass isotopes, and the solid triangles are obtained by doing number projection as well.

Arseniev, Sobiczewski, and Soloviev,[4] but we do not include any A dependence in this strength. The results are compared to experiment[21,22] in Figs. 4 and 5. As in the case of the Sn isotopes, three-quasiparticle configurations appear at ener-
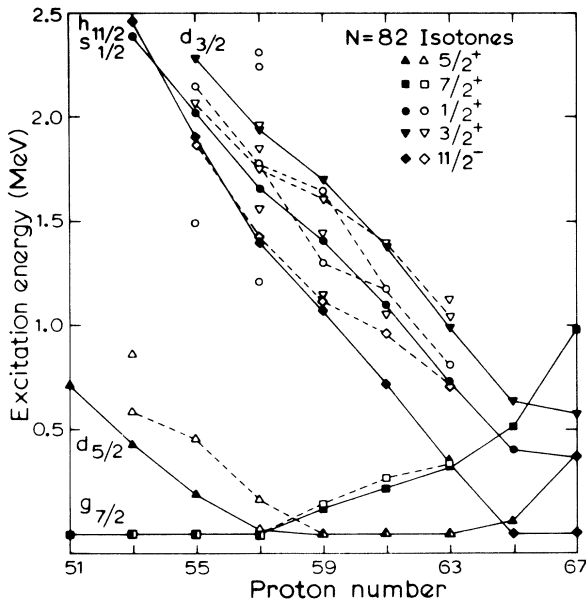

FIG. 4. The one proton quasiparticle states in the $N=82$ isotones. The open symbols are experimental levels, and the dashed lines join those levels which are observed to carry most of the proton stripping strength. The solid symbols joined by solid lines are the results of the BCS calculation with blocking.
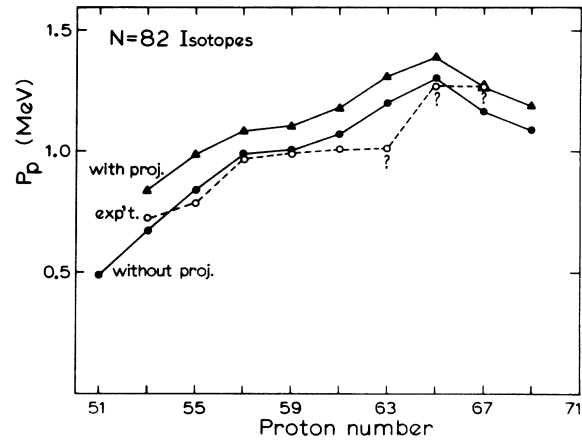

FIG. 5. The odd-even mass differences for the $N=82$ isotones. The open circles joined by a dashed line are the experimental results. The solid circles represent the results of the BCS calculation including blocking for the odd-mass isotones and the solid triangles are obtained by doing number projection as well. The experimental points that are accompanied by a question mark were obtained from separation energies listed in the Wapstra-Gove tables (Ref. 20) as derived from systematics.

gies $\gtrsim 1$ MeV. In all these nuclei, the lowest $\frac{5}{2}^+$, $\frac{7}{2}^+$, and $\frac{11}{2}^-$ levels have been experimentally established to be good one-quasiparticle states; however, this is not the case for the $\frac{1}{2}^+$ and $\frac{3}{2}^+$ levels; we have therefore indicated the position of the centroids of the $2s_{1/2}$ and $1d_{3/2}$ orbital as deduced from the (^{3}He, d) reaction.[21] It can, therefore, be concluded that the agreement between calculation and experiment is good, except for the $0h_{11/2}$ quasiparticle which comes too low in ^{143}Pm and ^{145}Eu, although it is correctly given in the lighter isotones.

At this point all the parameters of the effective Hamiltonian are determined, and all subsequent results are direct consequences of the models and the Hamiltonian. We continue this section with the study of the spherical nuclei near the closed proton or neutron shell, and turn to the deformed nuclei in the next section.

Some further results come directly out of the BCS calculations already discussed. First, the calculated occupation probabilities v_j^2 can be compared to experiment[9,21,23]; the agreement is good, the deviations being of the same general magnitude as those reported by others,[9] and comparable to the uncertainties in the extraction of v_j^2 from the experimental data. Secondly, the energies of the single neutron hole states in the $N=81$ isotones are directly given by the BCS calculation for the even $N=82$ isotones. These are compared to

experiment in Fig. 6; there are many states ob-
served above 1.2 MeV which are not shown, and
the calculated $1d_{5/2}$ and $0g_{7/2}$ hole states come
near 2.5 MeV, off the scale of the figure. The
first three levels are experimentally known[24] to
be reasonably pure $S_{1/2}$, $d_{3/2}$, and $h_{11/2}$ single
hole states, and our calculation predicts their
positions quite well. The $d_{5/2}$ and $g_{7/2}$ neutron
pickup strength, on the other hand, are very
fragmented, and less than 50% of the total
strength is observed below 2 MeV, which is where
the data stop. It is therefore reasonable to expect
the $1d_{5/2}$ and $0g_{7/2}$ centroids to lie in the 2 → 3 MeV
region where our calculation places them.

The single proton particle levels in the Sb iso-
topes can be obtained by using the BCS wave
functions for the even Sb isotopes, and the results
are shown in Fig. 7. We again only show the
lowest experimental states of each spin, and note
that there are many other levels above 0.9 MeV.
The first two levels are again known to be reason-
ably pure $0g_{7/2}$ and $1d_{5/2}$ states, and the calcula-
tion reproduces their positions quite well for
$A > 119$, but less well for the lighter isotopes.
The $2s_{1/2}$ and $1d_{3/2}$ stripping strengths are very
much fragmented,[25,26] so that the calculated po-
sition of these orbitals is not unreasonable. The
situation regarding the $h_{11/2}$ orbital is less clear:
the data of Ishimatsu et al.[25] suggest that the ob-
served state near 1.5 MeV is a very pure single
particle state, which would imply that our calcu-

lation puts this state about 1 MeV too high. On
the other hand the data of Conjaud, Harar, and
Cassagnov[26] put only half the stripping strength
in this state, with the remainder missing, and the
unified model calculations of Vanden Berghe and
Heyde[27] split the $h_{11/2}$ strength between the state
near 1.5 MeV and another state above 3.0 MeV in
roughly equal proportions. If the latter picture is
correct, then our $h_{11/2}$ orbital is still somewhat
high, but not unreasonably so.

From the above discussions, we conclude that
the single neutron energies, obtained from the Sn
spectra, are compatible with the data on the $N = 81$
isotones, and, similarly, that the single proton
energies required by the odd-mass $N = 82$ isotones
are compatible with the data on the Sb isotopes.

We conclude this section by mentioning in out-
line the results of a two-quasiparticle Tamm-
Dancoff calculation for the spectra of the even-
mass $N = 82$ isotones and Sn isotope. The general
trend of the data is reproduced and the individual
level positions are correct to 200 keV; this is
adequate, but somewhat worse than other similar
calculations which work in larger valence
spaces[9,10] or which allow some adjustment of the
parameters from one nucleus to the next.[11] We
note that the position of the 2^+ state is systemat-
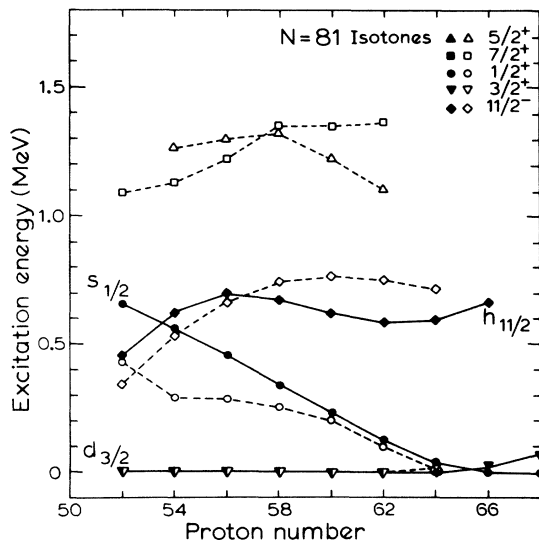
FIG. 6. The neutron hold states in the $N = 81$ isotones.
The solid symbols refer to theory and the open symbols
to experiment. The states just above 1 MeV do not
carry much neutron pickup strength and the large number
of states observed above these is not shown.
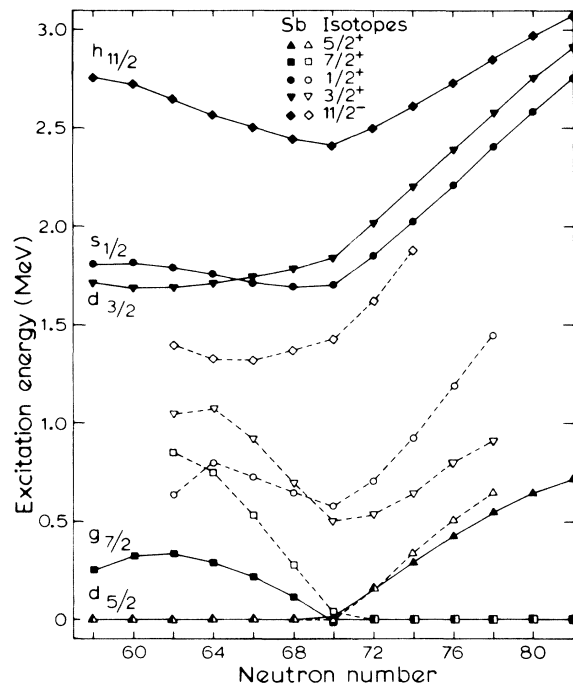

FIG. 7. The single proton states in the Sb isotopes.
The solid symbols refer to theory and the open symbols
to experiment. Only the lowest experimental levels of
each spin are shown.

ically too high, which is to be expected for a collective state described in a restricted valence space.

The calculated $B(E2)$ values can be compared to experiment[28,29] in order to determine the effective changes for our valence space. These are deduced to be $e_p = 1.7$ and $e_n = 1.1$; these values will be used in the subsequent sections.

IV. MODIFICATIONS OF CALCULATED RESULTS DUE TO NUMBER PROJECTION

If $|\phi\rangle$ is a wave function which is a superposition of wave functions of different particle numbers

$$|\phi\rangle = \sum_N a_N |\psi_N\rangle ,$$

then

$$a_N{}^2 = \frac{1}{2\pi} \int_0^{2\pi} e^{iN\theta} \langle\phi|e^{-i\hat{N}\theta}|\phi\rangle d\theta \qquad (2)$$

and

$$E_N = \langle\psi_N|H|\psi_N\rangle$$

$$= \frac{1}{2\pi a_N{}^2} \int_0^{2\pi} e^{iN\theta} \langle\phi|He^{-i\hat{N}\theta}|\phi\rangle d\theta. \qquad (3)$$

In Eqs. (2) and (3) $\hat{N}$ is the number operator.

The spectrum obtained from a blocking calculation is compared with that obtained from blocking and subsequent projection in Fig. 8. The differences are small enough so that in the bulk part of the paper unprojected results have been shown.

The effect of number projection on odd-even mass differences is shown in Figs. 3 and 5. In the Sn isotopes number projection lowers the odd-even mass differences, but in the $N = 82$ isotones it increases them. A likely reason for these two qualitatively different results is the following. If we parametrize the binding energies of the even-even nuclei by $E(N) = E_0 + AN + BN^2$, then, with our forces and single particle energies, the quantity B is negative for the Sn isotopes, but, because of the additional Coulomb force, B is positive for $N = 82$ isotones. The various implications of this parametrization of $E(N)$ have been discussed in a recent paper, where an approximate closed expression for $a_N{}^2$ was also derived by analogy with statistical mechanics.[30]

The effect of number projection on spectroscopic factors was also investigated. For the cases where the spectroscopic factors are significantly large, the effect is negligible.
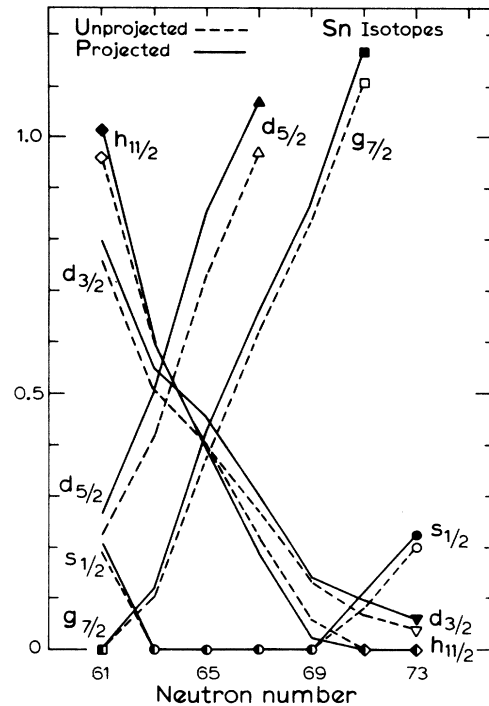

FIG. 8. The calculated spectrum of the neutron quasi-particle states in the Sn isotopes obtained with and without number projection.

V. SHAPE AND STRUCTURE OF THE NEUTRON-DEFICIENT Ba ISOTOPES

The matrix elements and single particle energies defined in Secs. II and III are in principle applicable to the whole $50 < N$, $Z < 82$ region. In this section we use them to study the light, neutron-deficient, even-even Ba isotopes, which are known to be moderately deformed. The experimental data, in particular the studies on the adjacent La isotopes,[1] show quite conclusively that the deformation is prolate. Much of the theoretical work, however, indicates a preference for oblate shapes,[3,4] although the predicted shapes are quite soft with regard to γ vibrations, and triaxial shapes can also be obtained.[5-8]

We use the following formalism. First, an axially symmetric, deformed, Hartree-Fock (HF) calculation is done, which generates a set of deformed orbitals

$$a^\dagger_{nk\mu} = \sum_j c^{k\mu}_{nj} a^\dagger_{jk\mu} , \qquad (4)$$

where k, μ are the z components of angular momentum and isospin, n labels the deformed orbitals with the same k and μ, and $a^\dagger_{jm\mu}$ creates a particle in a spherical shell model orbital. The

HF program requires that the number of particles with a given k and μ be fixed by the input; this makes it easy to generate both oblate and prolate solutions, and also to investigate different solutions which differ in the occupation of two levels near the Fermi surface, and which consequently have nearly equal energies.

The HF wave functions are then used in a BCS calculation (completely analogous to the spherical BCS calculation discussed in a previous section) which generates quasiparticle states

$$\alpha^\dagger_{nk\mu} = u_{nk\mu}a^\dagger_{nk\mu} - v_{nk\mu}a_{n\bar{k}\mu} .\tag{5}$$

Once the u's and v's are found, the ground state energy is calculated according to the formula

$$E_0 = \sum_{jk\mu n} \epsilon_{jk\mu}c^{k\mu}_{nj}c^{k\mu}_{nj}v_{nk\mu}{}^2$$

$$+\tfrac{1}{2}\sum_{\mu\mu'nkn'k'} v^{(a)}_{nk\mu n'k'\mu'nk\mu n'k'\mu'}v_{nk\mu}{}^2 v_{n'k'\mu'}{}^2$$

$$+\tfrac{1}{4}\sum_{\mu nkn'k'} v^{(a)}_{nk\mu n\bar{k}\mu n'k'\mu n'\bar{k}'\mu}u_{nk\mu}v_{nk\mu}u_{n'k'\mu}v_{n'k'\mu} .$$

$$\tag{6}$$

This procedure will be called the HFBCS method. The fully self-consistent calculation would require that we repeat the HF step with fixed $v_{nk\mu}$, then repeat the BCS step, etc., until convergence is achieved; however, with our present programs, this would be too expensive for the relatively minor changes that are expected to occur.

Once the HFBCS solution has been generated, it is used to obtain certain nuclear properties which can then be compared to experiment. Both the proton and the neutron quadrupole moments of the intrinsic state are calculated in a straight-forward way:

$$Q = \sum_{nk}\sqrt{\tfrac{16\pi}{5}}(nk\mu|r^2Y_{20}|nk\mu)v_{nk\mu}{}^2 ,\tag{7}$$

the summation being restricted to either protons or neutrons. According to the strong coupling model, these quadrupole moments are related to the transition rate from the bandhead to the first 2^+ state by[31]

$$B(E2)\!\uparrow = (5/16\pi)(e_pQ_p + e_nQ_n)^2 ,$$

where e_p and e_n are the proton and neutron effective changes. This relation is useful since the $B(E2)$ values in this region are fairly well known.[28]

The moment of inertia of the intrinsic state is calculated using the Nilsson-Prior[32] formalism

$$\mathcal{J} = \frac{1}{\hbar^2}\sum_{nkn'k'\mu}\frac{|\langle nk\mu|J_x|n'k'\mu\rangle|^2}{E_{nk\mu} + E_{n'k'\mu}} ,\tag{8}$$

where the $E_{nk\mu}$ are the quasiparticle energies. In

practice it is more convenient to talk about the moment of inertia parameter $A = \hbar^2/2\mathcal{J}$ than about the moment of inertia itself. One must be a little cautious when comparing this with experiment since the members of the ground state band do not follow a strict $J(J+1)$ scale. We therefore define an experimental moment of inertia factor as a function of J

$$A^{\text{exp}}_J = \frac{E_J - E_{J-2}}{4J - 2}\tag{9}$$

and compare the theoretical value to A^{exp}_J with $J \approx (\langle J^2\rangle)^{1/2}$, where $\langle J^2\rangle$ is the Hartree-Fock ground state expectation value of the operator J^2.

The results for the isotopes $^{126,\cdots,132}_{56}\text{Ba}$, and also for the $N = 72$ isotones $^{126}_{54}\text{Xe}$ and $^{130}_{58}\text{Ce}$, are shown in Table III. The principal result is that the prolate shape is energetically favored in all these nuclei. The prolate-oblate energy difference is substantial in the $^{126,128,130}\text{Ba}$ isotopes (>1.3 MeV), but somewhat less in ^{132}Ba and ^{130}Ce (~0.9 Mev) and smaller still in ^{126}Xe (~0.6 MeV). The predicted moments of inertia are in very good agreement with experiment for all the Ba isotopes and for ^{130}Ce, but not for ^{126}Xe. Using the effective charges determined from the Sn isotopes and the $N = 82$ isotones, and the quadrupole moments given by the HFBCS calculation, we get excellent agreement between the calculated and experimental $B(E2)\!\uparrow$ values for ^{126}Ba and ^{128}Ba, but the theoretical transition rate does not decrease with increasing neutron numbers as fast as the experimental rate. Similarly, the theoretical $B(E2)\!\uparrow$ in ^{126}Xe is about 25% too high.

Table IV gives a detailed description of the prolate HF and HFBCS solutions for ^{128}Ba. The most remarkable aspect of these solutions is the enormous gap (~2 MeV) between the occupied and empty proton orbitals. Because of this gap, there are no pairing correlations on the proton side. There is an analogous gap on the neutron side between the third and fourth orbitals, but of course these are far below the Fermi level, and the neutrons are superconducting with a modest (<0.9 MeV) pairing gap. There are only two low-lying proton particle orbitals near the Fermi level and these have $k = \tfrac{5}{2}^+$ and $\tfrac{3}{2}^+$, respectively.

The prolate solutions for the other Ba isotopes are very similar; in particular, the order of filling of the neutron orbitals is that implied in Table IV. The Hartree-Fock gap on the proton side decreases from 2.3 MeV in ^{126}Ba to 1.7 MeV in ^{132}Ba, and weak proton pairing correlations begin to appear in the last isotope.

The case of ^{132}Ba is also interesting because it allows us to test the accuracy of the HFBCS meth-

TABLE III. Summary of results for some neutron-deficient $Z=56$ isotopes and $N=72$ isotones. The various quantities are defined in the text. The values of $B(E2)\uparrow$ were calculated using $\hbar/m\omega=5.0$ fm^2, $e_p=1.7$, and $e_n=1.1$.

Nucleus	shape	E_{HF} (MeV)	E_{HFBCS} (MeV)	$\langle J^2 \rangle_{HF}$	A (MeV)	A_6 exp (MeV)	A_8 exp (MeV)	Q_p ($\hbar/m\omega$)	Q_n ($\hbar/m\omega$)	$B(E2)$ theory (e^2b^2)	$B(E2)$ exp (e^2b^2)
^{126}Ba	Prolate	−80.16	−80.69	65	0.027	0.028	0.025	28.4	35.6	1.92	2.02±0.33
	Oblate	−78.79	−79.43	69	0.032						
^{128}Ba	Spherical		−82.00								
	Prolate	−87.37	−87.80	58	0.028	0.029	0.026	28.3	32.8	1.78	1.63±0.35
	Oblate	−84.45	−86.00	72	0.041						
^{130}Ba	Prolate	−93.92	−94.67	50	0.029	0.031	0.027	27.6	27.3	1.50	1.09±0.16
	Oblate	−90.55	−93.12	67	0.056						
^{132}Ba	Prolate 1	−100.37	−101.43	47	0.038	0.037	?	26.0	20.8	1.16	0.72±0.18
	Prolate 2	−100.29	−101.43	39	0.045			24.0	21.2	1.04	
	Oblate	−97.83	−100.50	63	0.075						
^{126}Xe	Prolate	−64.62	−66.29	53	0.045	0.032	0.027	19.5	28.6	1.05	0.78±0.05
	Oblate	−63.79	−65.66	52	0.058						
^{130}Ce	Prolate	−105.90	−106.75	58	0.031	0.028	0.024	30.2	34.1	1.99	?
	Oblate	−104.22	−105.89	84	0.031						

od by comparing the results obtained starting from two different HF solutions. One solution (prolate 1) has the top $k=\frac{1}{2}^+$ neutron orbital occupied and the $k=\frac{9}{2}^-$ orbital empty, while the other solution (prolate 2) reverses this. In both cases, all the occupied levels come below all the empty levels so that both are good HF solutions, with their energies differing by 80 keV. The subsequent BCS calculation completely eliminates this difference, and the two quadrupole moments are also very close. The different ordering of the orbitals near the Fermi surface persists and since the Nilsson-Prior formula is unduly sensitive to energy spacings, there is a noticeable (~15%) change in the calculated moments of inertia. From this example, and a few others, we conclude that the HFBCS method is adequate for our purposes, and that a fully self-consistent calculation would not change the predicted intrinsic state energies by more than 100 keV.

The solutions for the other two $N=72$ isotones studied are again precisely what would be surmised from Table IV. In ^{126}Xe the lowest proton orbital is fully occupied, the next two orbitals ($k=\frac{3}{2}^+$ and $k=\frac{1}{2}^+$) have $v\approx 0.7$, and the remaining orbitals are empty. In ^{130}Ce, the lowest three proton orbitals are fully occupied, with the remaining two protons smeared out over the next four orbitals. The neutrons occupy the same orbitals in all the three $N=72$ isotones studied.

Table V gives a detailed description of the oblate HF and HFBCS solutions for ^{128}Ba. The oblate solutions for the other nuclides studied are basically similar.

A severe test for the deformed orbitals calcu-

lated in the HFBCS model can be obtained by considering odd-particle spectra. From the theoretical point of view the case of La will be simple, since its spectrum will be generated by one proton outside the closed proton core of Ba. A detailed calculation of La spectrum and comparison with experiment is made in the next section.

VI. SPECTROSCOPIC CALCULATIONS FOR ODD-MASS LANTHANUM ISOTOPES

The known low-lying levels in odd-mass La isotopes are displayed in Fig. 9. A systematic trend is that the excitation energy of the $\frac{11}{2}^-$ level drops going from the heavier to lighter isotopes. No $E3$ or $M2$ transitions have been seen from the $\frac{11}{2}^-$ state in ^{127}La. This suggests that the $\frac{5}{2}^+$ and $\frac{7}{2}^+$ states occur above this level. In that event the decay modes available to the $\frac{11}{2}^-$ state would be an $M4$ transition to $\frac{3}{2}^+$ state (if it occurs below $\frac{11}{2}^-$) or β decay. Assuming spacings of the order seen in ^{129}La, the $M4$ transition would be strongly hindered compared to the β decay which has a half-life ≈ 5 min. These points are discussed in detail in Ref. 1.

Looking at the positive parity levels one sees that the excitation energy of the $\frac{5}{2}^+$ drops going from ^{129}La to ^{131}La. In ^{133}La, $\frac{5}{2}^+$ becomes the ground state. It has been suggested that it is plausible that one is seeing two bands, one based on $k=\frac{3}{2}^+$ and one on $k=\frac{5}{2}^+$. The relative spacings of these two bands are changing as neutrons are added.

Considering the proton orbitals (Table IV) obtained in our calculations on Ba isotopes, we find that indeed the only two low-lying positive parity

TABLE IV. Details of the prolate solution for ^{128}Ba. The second and third columns refer to the HF calculation, the occupied orbitals being marked with an asterisk, and the subsequent columns refer to the HFBCS calculation. The Fermi level is denoted by λ.

	k	ϵ_k	Q_k	ϵ_k	Δ_k	E_k	υ_k
Protons	$\frac{11}{2}^-$	-2.63	-5.00	-3.10			0
	$\frac{1}{2}^+$	-4.54	-3.62	-4.78			0
	$\frac{3}{2}^+$	-4.55	-3.66	-4.68			0
	$\frac{9}{2}^-$	-5.04	-2.27	-5.17			0
	$\frac{7}{2}^+$	-5.71	-3.67	-5.93			0
	$\frac{5}{2}^+$	-6.35	-3.47	-6.54			0
	$\frac{7}{2}^-$	-6.96	-0.09	-6.90			0
	$\frac{1}{2}^+$	-7.78	0.22	-7.66			0
	$\frac{5}{2}^-$	-8.11	1.55	-8.04			0
	$\frac{3}{2}^-$	-8.74	2.64	-8.69			0
	$\frac{5}{2}^+$	-8.87	-0.19	-8.69			0
	$\frac{1}{2}^-$	-9.02	3.18	-8.98			0
	$\frac{3}{2}^+$	-9.20	0.26	-9.07			0
	$\frac{3}{2}^+$	-11.53^*	3.40	-11.22			1.00
	$\frac{1}{2}^+$	-11.56^*	3.93	-11.32			1.00
	$\frac{1}{2}^+$	-12.46^*	6.81	-12.25			1.00
Neutrons ($\lambda = -3.49$)	$\frac{11}{2}^-$	-0.47	-5.00	-0.80	0.82	2.80	0.147
	$\frac{9}{2}^-$	-2.11	-2.27	-2.25	0.74	1.44	0.266
	$\frac{3}{2}^+$	-2.13	-3.58	-2.09	0.85	1.63	0.272
	$\frac{1}{2}^+$	-2.57	-3.54	-2.63	0.82	1.19	0.371
	$\frac{7}{2}^+$	-3.10	-3.67	-3.07	0.88	0.97	0.533
	$\frac{7}{2}^-$	-3.76^*	-0.09	-3.83	0.66	0.75	0.853
	$\frac{5}{2}^+$	-4.17^*	-3.44	-4.27	0.81	1.13	0.920
	$\frac{1}{2}^+$	-4.92^*	0.10	-4.83	0.67	1.50	0.973
	$\frac{5}{2}^-$	-5.01^*	1.55	-5.02	0.57	1.64	0.984
	$\frac{5}{2}^+$	-5.56^*	-0.23	-5.40	0.76	2.06	0.982
	$\frac{3}{2}^-$	-5.72^*	2.64	-5.73	0.52	2.30	0.994
	$\frac{1}{2}^-$	-6.02^*	3.18	-6.04	0.49	2.60	0.995
	$\frac{3}{2}^+$	-6.29^*	0.23	-6.23	0.68	2.82	0.993
	$\frac{3}{2}^+$	-8.13^*	3.34	-7.94	0.56	4.49	0.998
	$\frac{1}{2}^+$	-8.49^*	3.69	-8.33	0.52	4.87	0.999
	$\frac{1}{2}^+$	-9.88^*	7.08	-9.76	0.29	6.28	1.000

orbitals for La have $k = \frac{3}{2}^+$ and $k = \frac{5}{2}^+$. They also have the characteristic behavior; the $k = \frac{5}{2}^+$ orbital drops in energy with respect to the $k = \frac{3}{2}^+$ orbital as neutrons are added. It is thus tempting to do a quantitative calculation. The lowest negative parity orbital is $k = \frac{1}{2}^-$. However, it is well-known that the negative parity states are very strongly band mixed, thus it is not possible to guess the relative spacings of positive and negative parity orbitals from the value of $\epsilon_{k=1/2}$.

In order to do a quantitative calculation we write

$$H = H_{\text{core}} + \epsilon_k,$$

where the ϵ_k's are obtained from our HFBCS cal-

TABLE V. Details of the solution for ^{128}Ba for oblate deformation (see Table III caption).

	k	ϵ_k	Q_k	ϵ_k	Δ_k	E_k	v_k
Protons ($\lambda = -10.04$)	$\frac{1}{2}^+$	-2.35	7.14	-3.07	0.32	6.98	0.023
	$\frac{1}{2}^-$	-4.55	3.18	-4.85	0.52	5.22	0.050
	$\frac{3}{2}^-$	-4.93	2.64	-5.17	0.54	4.90	0.055
	$\frac{1}{2}^+$	-5.41	3.41	-5.73	0.47	4.33	0.054
	$\frac{3}{2}^+$	-5.70	3.05	-5.92	0.50	4.15	0.060
	$\frac{5}{2}^-$	-5.83	1.55	-5.87	0.58	4.21	0.070
	$\frac{7}{2}^-$	-7.07	-0.09	-7.01	0.65	3.10	0.105
	$\frac{1}{2}^+$	-8.12	-0.01	-8.18	0.64	1.96	0.165
	$\frac{3}{2}^+$	-8.54	0.15	-8.60	0.62	1.57	0.200
	$\frac{9}{2}^-$	-8.72	-2.27	-8.49	0.74	1.71	0.222
	$\frac{1}{2}^+$	-9.27	-3.19	-9.19	0.84	1.20	0.381
	$\frac{5}{2}^+$	-9.42	-0.55	-9.23	0.62	1.02	0.323
	$\frac{3}{2}^+$	-9.73	-3.20	-9.43	0.86	1.05	0.458
	$\frac{11}{2}^-$	-10.74^*	-5.00	-10.26	0.88	0.91	0.788
	$\frac{5}{2}^+$	-10.99^*	-3.12	-10.74	0.81	1.07	0.909
	$\frac{7}{2}^+$	-12.79^*	-3.67	-11.91	0.92	2.08	0.974
Neutrons ($\lambda = -3.47$)	$\frac{1}{2}^+$	-0.57	6.88	-1.01	1.00	2.66	0.191
	$\frac{1}{2}^-$	-2.30	3.18	-2.58	0.81	1.21	0.359
	$\frac{3}{2}^-$	-2.57	2.64	-2.81	0.82	1.06	0.430
	$\frac{1}{2}^+$	-2.82	3.32	-3.12	0.98	1.04	0.576
	$\frac{3}{2}^+$	-2.90	2.85	-3.07	1.02	1.10	0.561
	$\frac{5}{2}^-$	-3.04^*	1.55	-3.28	0.82	0.84	0.621
	$\frac{7}{2}^-$	-3.98^*	-0.09	-4.06	0.76	0.96	0.898
	$\frac{1}{2}^+$	-5.10^*	0.28	-5.07	0.86	1.81	0.969
	$\frac{9}{2}^-$	-5.43^*	-2.27	-5.32	0.61	1.94	0.987
	$\frac{3}{2}^+$	-5.47^*	0.25	-5.52	0.88	2.22	0.979
	$\frac{5}{2}^+$	-6.21^*	-0.25	-5.95	0.95	2.65	0.983
	$\frac{1}{2}^+$	-6.49^*	-3.15	-6.45	0.54	3.02	0.996
	$\frac{3}{2}^+$	-6.79^*	-3.10	-6.49	0.62	3.08	0.995
	$\frac{11}{2}^-$	-7.85^*	-5.00	-7.34	0.41	3.89	0.999
	$\frac{5}{2}^+$	-7.92^*	-3.42	-7.76	0.56	4.32	0.998
	$\frac{7}{2}^+$	-9.37^*	-3.67	-8.56	0.71	5.14	0.998

culation. The basis vectors are

$$|IMk\rangle = \left(\frac{2I+1}{16\pi^2}\right)^{1/2}\left(D_{Mk}^{I*}(\Omega)R(\Omega)a_k^\dagger|\Phi_{\text{core}}\rangle\right.$$

$$\left. + (-)^{I-k}D_{M-k}^{I*}(\Omega)R(\Omega)a_{\bar{k}}^\dagger|\Phi_{\text{core}}\rangle\right).$$

$$(10)$$

Our D functions are those of Rose[33]; $|\Phi_{\text{core}}\rangle$ is the intrinsic state of the even-even core, and $a_{\bar{k}}^\dagger = e^{-i\pi j_y}a_k^\dagger$. The standard prescription is to write

$$H_{\text{core}} = A\vec{R}_e^2$$

$$= A(\vec{I}^2 + \vec{j}^2 - 2I_z j_z - I_+ j_- - I_- j_+),\qquad(11)$$

and then obtain the matrix elements of H_{core},

which leads to the usual band mixing formulas. Unfortunately, the Ba spectra are only quasirotational, so that $AJ_c(J_c+1)$ gives a rather poor fit which is not sufficiently improved by adding a $BJ_c^2(J_c+1)^2$ term. We therefore adopt a different procedure.

Consider the weak coupling basis in which H_{core} is diagonal:

$$|jJ_cIM\rangle = \sum_m (jJ_cmM-m|IM)\left(\frac{2J_c+1}{8\pi^2}\right)^{1/2} D_{M-m0}^{J_c*}(\Omega)a_{jm}^\dagger R(\Omega)|\Phi_{core}\rangle .\tag{12}$$

Using Eq. (4) and the recoupling properties of the D matrices, the basis vector $|IMk\rangle$ of Eq. (10) can be expressed in terms of $|jJ_cIM\rangle$ of Eq. (12):

$$|IMk\rangle = \frac{1}{[2(2I+1)]^{1/2}} \sum_{jJ_c} c_{jk}(2J_c+1)^{1/2}(jJ_ck\,0|Ik)[1+(-)^{J_c}]|jJ_cIM\rangle .\tag{13}$$

Using the above expansion we find

$$\langle IMk|H_{core}|IMk'\rangle = \frac{1}{2I+1}\sum_{jJ_c}(2J_c+1)(jJ_ck\,0|Ik)(jJ_ck'\,0|Ik')c_{jk}c_{jk'}[1+(-)^{J_c}]E_{J_c} .\tag{14}$$

The advantage of Eq. (14) is that the values of the core energy E_{J_c} can be directly used. The summation in Eq. (14) is restricted to $J_c \leqslant |I+j_{max}|$. One can verify that for $E_{J_c}=AJ_c(J_c+1)$ the usual band mixing and decoupling terms are obtained.[34]

We now use Eq. (14) to study the negative parity levels of the odd-mass La isotopes in the spins up to $I=\frac{23^-}{2}$. Since $j=\frac{11^-}{2}$, this requires the values of E_{J_c} for $J_c \leqslant 16$; these have been experimentally determined only for $J_c \leqslant 10$, so that the remainder was obtained by extrapolation from the observed positions of the 6$^+$, 8$^+$, and 10$^+$ levels. All k values are allowed to mix, and the results of the calculation are shown in Fig. 10. The agreement

with experiment is excellent. Previous calculations[1,35,36] have also been very successful for this set of states, provided that prolate deformations were assumed.

The positive parity levels are expected to arise from the $k=\frac{3^+}{2}$ and $k=\frac{5^+}{2}$ bands. Since these are close in energy they will be band mixed. In this case we only need the values of E_{J_c} with $J_c\leqslant 10$, which are all known. The relative positions of $I=\frac{11^-}{2}$ and $I=\frac{3^+}{2}$ calculated using our computed ϵ_k's are shown in Fig. 9. As in experiment, our calculations show that the excitation energy of $\frac{11^-}{2}$ increases as neutrons are added; the calculated increase is not, however, fast enough.
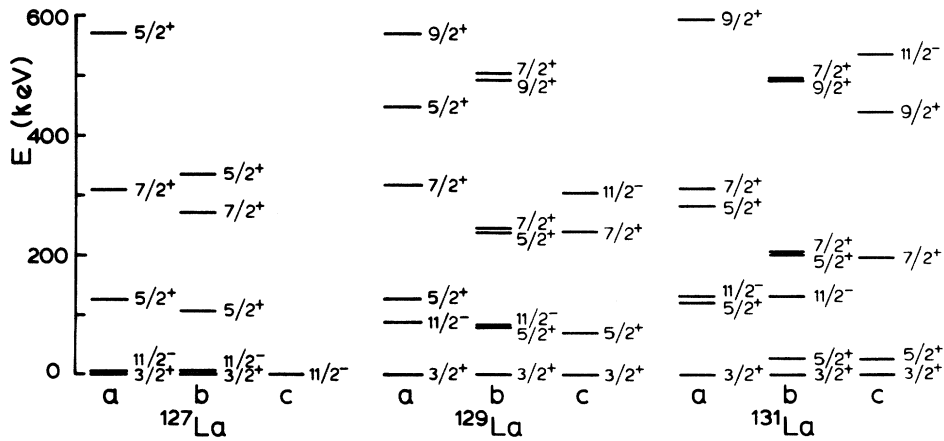

FIG. 9. Low lying levels in the odd-mass La isotopes. The spectrum labeled c is experimental, the spectrum labeled a is obtained by band mixing using the HFBCS single proton energies, and the spectrum labeled b is obtained by band mixing with the $k=\frac{5^+}{2}$ proton orbital energy lowered by a constant 255 KeV in all the nuclei.

To get good agreement with the positions of the $\frac{5}{2}^+$, $\frac{7}{2}^+$, and $\frac{9}{2}^+$ levels some adjustment of $\epsilon_{k=3/2}$ or $\epsilon_{k=5/2}$ is necessary. If these are taken from our HFBCS calculation, the lowest $\frac{5}{2}^+$ is predominantly $k = \frac{3}{2}^+$. Experimentally, in ^{131}La the $\frac{5}{2}^+$ state is only 26 keV above the $\frac{3}{2}^+$. Such a small excitation energy cannot be obtained in a pure k band since its spectrum is entirely determined by the energy spacings in ^{130}Ba. This state cannot be pure $k = \frac{5}{2}^+$ either, since the $|\frac{5}{2}^+, k = \frac{3}{2}\rangle$ state must be in the immediate vicinity and must perturb it strongly.

The energy levels obtained when $\epsilon_{k=5/2^+}$ is lowered by a constant 255 keV in all the La isotopes from that obtained in the HFBCS calculations are also shown in Fig. 9. The agreement with the known positive parity energy levels is now quite good. Compared to experiment, we have an extra $\frac{5}{2}^+$ and an extra $\frac{7}{2}^+$ in ^{131}La. We will return to their discussion shortly, but first let us discuss some known electromagnetic transition rates in ^{131}La. All the experimental data quoted are from Ref. 1.

The $\frac{7}{2}^+ \to \frac{5}{2}^+$ transition is known to be predominantly $M1$. In our calculation we find $T(M1, \frac{7}{2} \to \frac{5}{2})/T(E2, \frac{7}{2} \to \frac{5}{2}) = 10$. The experimental ratio for $T(M1, \frac{7}{2} \to \frac{5}{2})/T(E2, \frac{7}{2} \to \frac{3}{2})$ is 20; our calculated value is 42. It has been noted that the quantity $R \equiv T(E2, \frac{9}{2} \to \frac{5}{2})/T(M1, \frac{9}{2} \to \frac{7}{2})$ is large in these La

isotopes; $R_{\text{exp}}/R_{\text{s.p.}}$ in ^{131}La is 800. It has been suggested that a "spherical" model will be needed to explain this high ratio. In this spherical model the $\frac{9}{2}^+$ is viewed as a $d_{5/2}$ particle coupled to a 2+ phonon and the $\frac{7}{2}^+$ state is essentially a $g_{7/2}$ particle state. While such a model will obviously lead to a high value of R due to l forbiddenness of $M1$ transitions, we find a large value of $R = 518$ is also obtained in our calculation. Such a high value is obtained in our calculations for two reasons: the $\frac{9}{2}^+ \to \frac{5}{2}^+$ $E2$ transition, being of a collective nature, is enhanced and we obtain $T(E2; \frac{9}{2} \to \frac{5}{2})/T_{\text{s.p.}}(E2; \frac{9}{2} \to \frac{5}{2}) \approx 25$; in addition, $T(M1; \frac{9}{2} \to \frac{7}{2})/T_{\text{s.p.}}(M1; \frac{9}{2} \to \frac{7}{2}) \approx 0.05$. Thus we find that electromagnetic transition rates are explained adequately in the deformed model.

In calculating transition rates we used standard formulas for rotational models for band mixed states; the core quadrupole moment was deduced from the $2^+ \to 0^+$ transition in ^{130}Ba. The value of g_R used was Z/A; $g_s = 5.58$ and $g_l = 1$.

The levels of ^{131}La have also been studied in the ^{130}Ba $(\alpha, t)^{131}$La reaction, although no spectroscopic factors are available. The $\frac{5}{2}^+$, $\frac{7}{2}^+$, and $\frac{11}{2}^-$ levels have been identified. In our calculation the spin $\frac{3}{2}^+$ is pure $k = \frac{3}{2}^+$; this $k = \frac{3}{2}^+$ has very little $d_{3/2}$ component in it and leads to a small spectroscopic factor $= 0.0047$. The lowest $\frac{5}{2}^+$ level has $S_{d_{5/2}}^2 = 0.015$, but unfortunately the contribution comes from two largely canceling terms originating from $k = \frac{3}{2}$ and $k = \frac{5}{2}$. This can alter the value by a factor of 4 without very significant changes in the mixing amplitudes. The lowest $\frac{7}{2}^+$ has a spectroscopic factor of 0.28, and the lowest $\frac{11}{2}^-$ has $S_{11/2}^2 = 0.53$.

The second $\frac{5}{2}^+$ obtained in our calculations arises because there are two bands. This has a spectroscopic factor of 0.26. On the other hand, in our calculation this is almost degenerate with the second $\frac{7}{2}^+$ and might not be resolved in the (α, t) experiment. The electromagnetic decay from the $\frac{9}{2}^+$ to the $\frac{5}{2}^+$ would also be unfavored compared with the known $\frac{9}{2}^+$ to $\frac{7}{2}^+$ decay. If it is conclusively resolved experimentally that no second $\frac{5}{2}^+$ exists among the low-lying levels of ^{131}La, that would imply that (a) $\epsilon_{k=5/2}$ is obtained too low in our HFBCS calculation, and (b) the strong coupling model does not give a good fit to the energies of the low-lying positive parity levels in ^{131}La. In particular, the energy of the lowest $\frac{5}{2}^+$ would be too high.
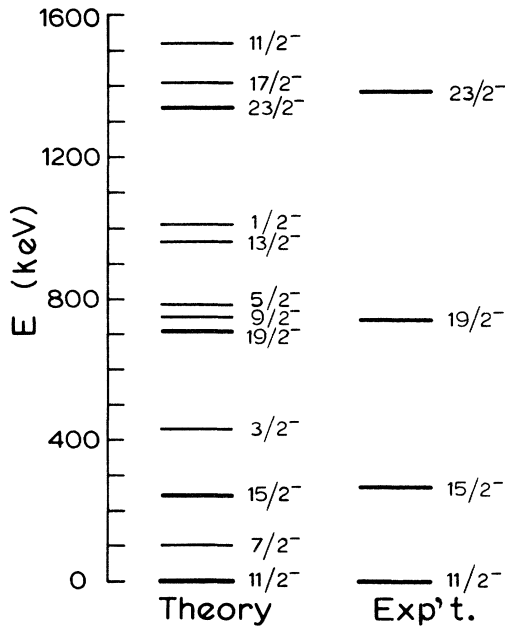

FIG. 10. The theoretical and experimental spectra of the the negative parity states in ^{129}La. The theoretical results are obtained by a band mixing calculation using the experimental energies of the ground band of ^{128}Ba.

VII. CONCLUSIONS

We conclude from the present work that it is possible to give a reasonably accurate description of the nuclei in the region of the Periodic Table

limited by 50< N, Z < 82 using a uniform set of single particle energies and semirealistic matrix elements. All the parameters are fixed by the data on the odd-mass N = 82 isotones and Sn isotopes. Prolate shapes are predicted to be clearly favored over oblate shapes for all the Ba isotopes studied (^{126}Ba to ^{132}Ba), and the calculated moments of inertia and $B(E2)$ values are in good agreement with the data. The energy levels and electromagnetic decay properties in the adjacent La isotopes are deduced and are shown to agree well with experiment, although some disagreement with the proton stripping data is noted.

Of course, it is possible that the nuclei in this deformed region actually have triaxial shapes; however, for the Ba isotopes, the substantial energy difference between prolate and oblate deformation and the good agreement with experi-

ment indicate that prolate shapes are at least a good first approximation. The situation may be somewhat different for the Xe or Ce isotopes.

It is a straightforward matter to extend these calculations to other nuclei in this region. However, before doing this, it may be advantageous to generate a better set of nuclear matrix elements. In particular, a reasonable A dependence should be included, and the treatment of the core-polarization corrections should be improved by including a collective octupole bubble.

ACKNOWLEDGMENTS

*Work supported in part by the National Research Council of Canada.

[1]J. R. Leigh, K. Nakai, K. H. Maier, F. Pühlhofer, F. S. Stephens, and R. M. Diamond, Nucl. Phys. A213, 1 (1973).

[2]K. Nakai, P. Kleinheinz, J. R. Leigh, K. H. Maier, F. S. Stephens, R. M. Diamond, and G. Løvhøiden, Phys. Lett. 44B, 443 (1973).

[3]K. Kumar and M. Baranger, Phys. Rev. Lett. 12, 73 (1964).

[4]D. A. Arseniev, A. Soliczewski, and V. G. Soloviev, Nucl. Phys. A126, 15 (1969).

[5]I. Ragnarsson, A. Sobiczewski, R. K. Sheline, S. E. Larsson, and B. Nerlo-Pomorska, Nucl. Phys. A233, 329 (1974).

[6]H. Flocard, P. Quentin, A. K. Kerman, and D. Vautherin, Nucl. Phys. A203, 433 (1973).

[7]S. G. Rohozinski, J. Srebrny, and K. Horbaczewska, Z. Phys. 268, 401 (1974).

[8]D. Habs, H. Klewe-Nebenius, K. Wisshak, R. Löhker, G. Nowicki, and H. Rebel, Z. Phys. 267, 149 (1974).

[9]E. Baranger, in Advances in Nuclear Physics, Vol. 4 edited by M. Baranger and E. Vogt (Plenum, New York, 1971).

[10]H. C. Lee and K. Hara, Phys. Rev. C 3, (1971) 325; H. C. Lee (private communication).

[11]M. Waroquier and K. Heyde, Nucl. Phys. A144, 481 (1970); A164, 113 (1971); Z. Phys. 268, 11 (1974).

[12]D. Larson, S. M. Austin, and B. H. Wildenthal, Phys. Rev. C 9, 1574 (1974); and (unpublished).

[13]F. Tabakin, Ann. Phys. (N.Y.) 30, 51 (1964).

[14]N. de Takacsy, Can. J. Phys. 46, 2091 (1968).

[15]G. Bertsch, Nucl. Phys. 74, 234 (1965).

[16]T. T. S. Kuo and G. E. Brown, Nucl. Phys. 85, 40 (1966).

[17]G. H. Herling and T. T. S. Kuo, Nucl. Phys. A181, 113 (1972).

[18]P. E. Cavanagh, C. F. Coleman, A. G. Hardacre,

E. A. Gard, and J. F. Turner, Nucl. Phys. A141, 97 (1970).

[19]D. Clement and E. U. Baranger, Nucl. Phys. A120, 25 (1968).

[20]A. H. Wapstra and N. B. Gove, Nucl. Data A9, 267 (1971).

[21]B. H. Wildenthal, E. Newman, and R. L. Auble, Phys. Rev. C 3, 1199 (1971).

[22]S. K. Mark (private communication).

[23]P. E. Cavanagh, AERE report, 1968 (unpublished), quoted in Ref. 9.

[24]A. Chaumeaux, G. Bruge, H. Faraggi, and J. Picard, Nucl. Phys. A164, 176 (1971).

[25]T. Ishimatsu, K. Yagi, H. Ohmura, Y. Nakajima, T. Nakagawa, and H. Orihara, Nucl. Phys. A104, 481 (1967).

[26]M. Conjeaud, S. Harar, and Y. Cassagnou, Nucl. Phys. A117, 449 (1968).

[27]G. Vanden Bergh and K. Heyde, Nucl. Phys. A163, 478 (1971).

[28]C. K. Ross and R. K. Bhaduri, Nucl. Phys. A196, 369 (1972).

[29]J. R. Kerns and J. X. Saladin, Phys. Rev. C 6, 1016 (1972).

[30]S. Das Gupta and N. de Takacsy, Nucl. Phys. A240, 293 (1975).

[31]S. G. Nilsson, K. Dan. Vidensk Selsk. Mat.-Fys. Medd. 29, No. 16 (1955).

[32]S. G. Nilsson, and O. Prior, K. Dan. Vidensk Selsk. Mat.-Fys. Medd. 32, No. 16 (1961).

[33]M. E. Rose, Elementary Theory of Angular Momentum (Wiley, New York, 1957).

[34]S. Das Gupta and N. de Takacsy, Am. J. Phys. (to be published).

[35]S. Das Gupta and N. de Takacsy, Phys. Rev. C 10, 1220 (1974).

[36]A. Ikeda, R. K. Sheline, and N. Onishi, Phys. Lett. 44B, 397 (1973).